Indian Journal of Pure & Applied Physics
Vol. 58, February 2020, pp. 87-98

Heat transfer in combined convective magnetohydrodynamic motion of nanofluid holding different shapes of nanoparticles in a channel under the influence of heat source

Pentyala Srinivasa Rao[a], Om Prakash[a,b] & Ram Prakash Sharma[c*]

[a]Department of Applied Mathematics, IIT (ISM), Dhanbad 826 004, India
[b]Department of Mathematics, JECRC University, Jaipur 303 905, India
[c]Department of Basic & Applied Science, National Institute of Technology Arunachal Pardesh, Yupia, Papum Pare 791 112, India

Received 18 January 2019; accepted 2 January 2020

Heat transfer in mixed convection unsteady MHD flow of an incompressible nanofluid in a channel under the influence of heat source is studied. The channel with non-uniform walls temperature is taken in a perpendicular direction with a transverse magnetic field. Based on the substantial boundary conditions, three different flow conditions are examined. The problem is formed in PDEs with substantial boundary conditions. Four different forms of nanoparticles of identical volume fraction are employed in traditional base fluid water (H_2O). Solutions for momentum and energy are attained by the perturbation method and examined graphically in different graphs. It is established that viscosity and thermal conductivity are the mainly well-known variables accountable for different results of velocity and temperature. It is also found that increasing heat source leads to an increase in nanofluid velocity and temperature and nano-size particles instance platelet and blade shapes have lesser momentum as related to brick and cylinder size of nanoparticles.

Keywords: Heat source, Combined convection, Nanofluid, MHD flow, Cylindrical-shaped nanoparticles

1 Introduction

A very important role is played by thermal conductivity in heat transfer enhancement. Conventional heat flows down after getting converted into various forms, for example, ethylene glycol, kerosene oil, lubricant oils, whereas solid are comparatively less transferrable. Fluids have a comparatively less thermal conductivity if we have to compare it with solids. Choi[1] in his pioneering work indicates that thermal conductivity is increased if commonly based fluids are added to a small number of nanoparticles. At the same time, it increases the heat transfer rate. These mixtures are generally called nanofluids. Particles of nano-size in base fluids are more exactly called nanofluids. Various kinds of nano-particles, for example, oxides, carbides, and metals in normally base fluids like water, EG, kerosene oil, and propylene glycol are usually contained in nanofluids. A choice of electronic apparatus, power generation, AC, energy supply and fabrication are specifically well equipped by the nanofluids application. Mansur *et al*.[2] have reported nanofluids for MHD stagnation point motion over a porous surface for extending and contracting cases. They gained mathematical results applying the bvp4c curriculum in MATLAB and evaluated outcomes in favor of immersed variables. The capacity of nanoparticles to increase the thermal conductivity of normal fluids jointly through many uses of nanofluids in engineering has to pay attention to the curiosity of investigators to carry out more investigations. Along with them, numerous are presenting hypothetical research, a number of them are applying computation methods, though especially only some investigations are accessible on the analytic face. Possibly, this is because of the cause that systematic explanations are not forever suitable. Amongst the diverse efforts is stated at this point individuals completed in references[3–13].

Both nanoparticles and their shapes decide the worth of the nanofluid. Scientist generally uses nanoparticles of spherical shapes. Though, concerning implementations and implication, spherical form nanoparticles are limited. Because of this cause, non-spherical form nanoparticles are taken in this investigation. Generally, 4-different kinds of nano-particles namely platelet, cylinder, brick, and blade are included in this investigation. Nanoparticles play a

*Corresponding author (E-mail: rpsharma@nitap.ac.in)

significant role in the present research particularly in cancer therapy and especially keep guiding the non-spherical in shaping nanoparticles. Recently, it has been revealed that nanoparticles are seven times dangerous when they occupy cylindrical shape. They also play a magnificent role in serving as drugs for breast cancer. Various shapes of nanoparticles in different fluids such as water have not yet been recorded.

The issue of aluminum oxide nanofluids holding unlike form nanoparticles however, they managed this work practically jointly by theoretical modeling has been examined by Timofeeva *et al.*[14]. Radiation impacts on an unsteady free convective motion of nanofluids past an infinite vertical sheet have been reviewed and spherical nanoparticles are examined by Loganathan *et al.*[15]. They accomplished that spherical copper (Cu), titanium dioxide (TiO_2) and aluminum oxide nanofluid momentum is greater than silver (Ag) spherical nanofluids because of superior viscosity. Asma *et al.*[16] have analyzed correct solutions for natural convective nanofluids motion in the presence of ramped wall temperature with considering 5 dissimilar kinds of spherical shaped nanoparticles. Energy transport because of convection occurs in numerous physical conditions.

Sebdani *et al.*[17] have examined the energy transport of aluminum oxide H_2O based nanofluid in assorted convective motion. The assorted convective energy transport in a parallel channel packed by nanofluids has been reported by Fan *et al.*[18]. The study of boundary layer motion assorted convective flow of a nanofluid has been analyzed by Tiwari and Das[19] and Sheikh Zadeh *et al.*[20]. Nadeem and Saleem[21] have reviewed the flow of unsteady of a revolving magnetohydrodynamic nano-fluid in a revolving cone. The magnetohydrodynamic assorted convective motion in a straight hot cavity has been analyzed by Al-Salem *et al.*[22]. The impacts of changeable thermal conductivity and viscosity on the magnetohydrodynamic motion and energy transport past an irregular extending sheet have been reported by Prasad *et al.*[23]. The issue of Darcy Forchheimer's assorted convective transport of energy and concentration in a flooded permeable medium has been examined by Rami *et al.*[24]. Influences of magnetic field and radiation on the assorted convective stagnation point motion past a vertically extending surface via a permeable medium surrounded by an extending vertical sheet have been evaluated by Hayat *et al.*[25]. A small number of other studies on assorted convective and nanofluids are given in references[26–36].

Ibrahim *et al.*[37] have examined the effect of thermal radiation and heat source/sink on the dissipative magnetohydrodynamic combined convective motion of a Casson nanofluid past a nonlinear porous stretching surface with chemical reaction, the effect of Brownian motion and thermophoresis and suction. Nandy and Mahapatra[38] have reported the influence of heat source/sink, velocity slip and Brownian motion and thermophoresis on magnetohydrodynamic stagnation point motion and energy transport past an extending sheet under the influence of convective boundary conditions. Hayat *et al.*[39] have studied the effect of nonlinear thermal radiation on melting heat transfer is a stagnation point motion of nanofluid to an extending sheet with an inclined magnetic field. Kundu *et al.*[40] have reported the influences of Brownian motion and thermophoresis, a uniform transverse magnetic field and internal heat source on the steady 2D motion of an electrically conducting nanofluid past a perpendicular convectively hot porous extending sheet in the presence of variable stream conditions. Das[41] has studied the effect of chemical reaction on steady magnetohydrodynamic boundary layer motion of nanofluid past a vertical convectively hot permeable extending surface under the influence of variable stream conditions. Madhu and Kishan[42] have analyzed the influence of heat source/sink and magneto-hydrodynamic on the boundary-layer motion of a Jeffrey fluid model for non-Newtonian nanofluid over an extending surface. Naramgari and Sulochana[43] have studied the influences transverse magnetic field, non-uniform heat source/sink, thermal radiation and suction on velocity and energy transport behavior of Jeffrey, Maxwell and Oldroyd-B nanofluids past an extending sheet.

Based on the above text, the current study is perturbed through the radiation transfer of heat in the combined convective magnetohydrodynamic motion of an unlike the size of Al_2O_3 in the water base nanofluid in a channel packed with flooded permeable media. The influence of diverse parameters on cylinder shape nanofluids has been paid much attention. The fluid is considered to be electrically conducting and it is very difficult to get it reviewed at the boundary of the channel. The present study emphasizes three different flow cases. The channel

both walls remain immovable in case first. The buoyancy force begins fluid flow jointly exterior pressure gradient of oscillatory form applied in the motion way. The channel upper wall is movable whereas the lower wall is stationary as per the second case and in the third case both walls of the channel are movable. The momentum and energy are gained through perturbation solutions and result in the surface of skin friction and Nusselt number is analyzed. Various parameters of interest are presented through the graphical results for momentum and energy distributions.

2 Mathematical Model and Solution

Let us consider the oscillatory motion of an incompressible nanofluid in an outlet packed through a saturated permeable medium. The influence of a magnetic field of strength B_0 applied in a crosswise direction to the flow has been assumed if the fluid is electrically conducted. The magnetic Reynolds play a significant role if induced magnetic field and it can be ignored to a small amount. It is assumed that the electric field is polarized and the exterior electric field is considered zero becomes useless. There is radiation effect in the energy equation whereas there is a no-slip situation at the boundary appears. It usually behaves that x–axis has a role along with the flow whereas y–axis plays its role in normal flow. When buoyancy force mutually with external pressure gradient applied along the x–direction, it creates the mixed convection. Under the normal condition of Boussinesq approximation, the governing equation of momentum and energy remains as given below (Aiza *et al.*[13] and Hamilton and Crosser[26]):

$$\rho_{nf} u_t = -p_x + \mu_{nf} u_{yy} - \left(\sigma B_0^2 + \frac{\mu_{nf}}{k_1}\right) u + (\rho\beta)_{nf}\, g(T - T^*) \quad \ldots (1)$$

$$\left(\rho c_p\right)_{nf} T_t = k_{nf} T_{yy} - q_y + Q_0 (T - T^*) \quad \ldots (2)$$

$$\mu_{nf} / \mu_f = 1 + a\phi + b\phi^2 \quad \ldots (3)$$

$$k_{nf} = \frac{k_f [k_s + (n-1)k_f + (n-1)(k_s - k_f)\phi]}{k_s + (n-1)k_f - (k_s - k_f)\phi} \quad \ldots (4)$$

Nanofluids thermal conductivity results[15,16] are given as:

$$\rho_{nf} = (1-\phi)\rho_f + \phi\rho_s,\ (\rho\beta)_{nf} = (1-\phi)(\rho\beta)_f + \phi(\rho\beta)_s,$$
$$(\rho c_p)_{nf} = (1-\phi)(\rho c_p)_f + \phi(\rho c_p)_s$$
. $\quad \ldots (5)$

The n occurring in Eq. 4 is the actual form factor specified through $n = 3/\psi$, the ratio among the sheet area of the sphere and the sheet area of the actual particle with the same volumes given by the sphericity ψ. The changed particle shape for the values[14] of ψ are given in Table 2.

Substantial characteristics of base fluid and nanoparticles are specified in Table 3 as mentioned by literature[15,16].

The radiative heat flux[29] is specified:

$$q_y = -4\alpha^2 (T - T^*) \quad \ldots (6)$$

Substituting value from Eq. (6) into Eq. (2), then we have:

$$\left(\rho c_p\right)_{nf} T_t = k_{nf} T_{yy} + 4\alpha^2 (T - T^*) + Q_0 (T - T^*) \quad \ldots (7)$$

The dimensionless variables introducing are as follows:

$$\tilde{x} = \frac{x}{d},\ \tilde{y} = \frac{y}{d},\ \tilde{u} = \frac{u}{U_0},\ \tilde{t} = \frac{tU_0}{d},\ \tilde{p} = \frac{d}{\mu U_0} p,$$
$$\tilde{T} = \frac{T - T^*}{T_w - T^*},\ \tilde{\omega} = \frac{d\omega}{U_0},\ \frac{\partial \tilde{p}}{\partial \tilde{x}} = \lambda e^{i\tilde{\omega}\tilde{t}} \quad \ldots (8)$$

Using Eq. (8) in Eqs (1 and 7), the dimensionless governing equations can be written as (neglecting the bars for convenience):

$$a_0 u_t = \lambda\varepsilon\, \mathrm{e}^{i\omega t} + \phi_2 u_{yy} - m_0^2 u + a_1 T \quad \ldots (9)$$

$$b_0^2 T_t = T_{yy} + b_1^2 T \quad \ldots (10)$$

Where,

$$\phi_1 = (1-\phi) + \phi\frac{\rho_s}{\rho_f},\quad \phi_2 = 1 + a\phi + b\phi^2,$$

$$\phi_3 = (1-\phi) + \phi\frac{(\rho\beta)_s}{(\rho\beta)_f},\quad \phi_4 = (1-\phi) + \phi\frac{(\rho c_p)_s}{(\rho c_p)_f}$$

$$\mathrm{Re} = \frac{U_0 d}{\nu_f},\ M^2 = \frac{\sigma B_0^2 d^2}{\mu_f},\ K = \frac{k_1}{d^2},\ a_1 = \phi_3 Gr,$$

$$Gr = \frac{g\beta_f d^2 (T_w - T^*)}{U_0 \nu_f},\ \varepsilon = -\frac{\mu}{\nu_f},\ a_0 = \phi_1 \mathrm{Re},$$

$$Pe = \frac{(\rho c_p)_f U_0 d^2}{k_f},\ N^2 = \frac{4d^2\alpha^2}{k_f},\ b_1^2 = \frac{N^2}{\lambda_n} + Q,$$

$$\lambda_n = \frac{k_{nf}}{k_f},\ Q = \frac{Q_0 d^2}{k_{nf}},\ b_0^2 = \frac{Pe\,\phi_4}{\lambda_n},\ m_0^2 = M^2 + \frac{\phi_2}{K}$$

From Eqs (9) and (10), we have taken the subsequent 3 different cases:

Case I: Motion inside a channel with immovable sheets.

In this case, the motion within a channel of width d packed with nanofluids is assumed and together sheets of the channel are immovable at $y = 0$ and $y = d$. The top sheet of the channel is supposed retained at a fixed temperature T_w and the bottom sheet has a constant temperature T^*. Therefore, the B. C's are

$$u(0,t) = 0, \qquad u(d,t) = 0 \qquad \ldots (11)$$

$$T(0,t) = T^*, \quad T(d,t) = T_w \qquad \ldots (12)$$

The boundary conditions (11) and (12) in the dimensionless form are:

$$u(0,t) = 0, \qquad u(1,t) = 0; \quad t > 0, \qquad \ldots (13)$$

$$T(0,t) = 0, \qquad T(1,t) = 1; \quad t > 0, \qquad \ldots (14)$$

Now, solve the Eqs (9) and (10) with boundary conditions (13) and (14), the perturbed solutions are taken of the forms:

$$u(y,t) = [u_0(y) + \varepsilon e^{i\omega t} u_1(y)], \qquad \ldots (15)$$

$$T(y,t) = [T_0(y) + \varepsilon e^{i\omega t} T_1(y)], \qquad \ldots (16)$$

for velocity and temperature, respectively.

Using Eqs (15 and 16), we have the Eqs from (17) to (22) as follows:

$$u_t(y,t) = \varepsilon i\omega e^{i\omega t} u_1(y) \qquad \ldots (17)$$

$$u_y(y,t) = u_0'(y) + \varepsilon e^{i\omega t} u_1'(y) \qquad \ldots (18)$$

$$u_{yy}(y,t) = u_0''(y) + \varepsilon e^{i\omega t} u_1''(y) \cdot \qquad \ldots (19)$$

$$T_t(y,t) = \varepsilon i\omega e^{i\omega t} T_1(y) \qquad \ldots (20)$$

$$T_y(y,t) = T_0'(y) + \varepsilon e^{i\omega t} T_1'(y) \qquad \ldots (21)$$

$$T_{yy}(y,t) = T_0''(y) + \varepsilon e^{i\omega t} T_1''(y) \qquad \ldots (22)$$

Putting the values from Eqs (17)-(19) in Eq. (9) and Eqs (20)-(21) in Eq. (10), we get the following ordinary differential equations are:

$$(D^2 - m_1) u_0(y) = -a_2 T_0(y), \qquad \ldots (23)$$

$$(D^2 - m_2) u_1(y) = \frac{-\lambda - a_1 T_1(y)}{\varphi_2}, \qquad \ldots (24)$$

$$(D^2 + b_1^2) T_0(y) = 0, \qquad \ldots (25)$$

$$(D^2 + m_3^2) T_1(y) = 0, \qquad \cdot\ldots (26)$$

Where $m_1 = m_0^2/\phi_2$, $\quad a_2 = a_1/\phi_2$,

$m_2 = \left(m_0^2 + i\omega a_0\right)/\phi_2$, $\quad m_3 = \sqrt{b_1^2 - b_0^2 i\omega}.$

The corresponding B.C's (13) and (14) are converted to:

$$u_0(0) = 0, \qquad u_0(1) = 0, \qquad \ldots (27)$$

$$u_1(0) = 0, \qquad u_1(1) = 0, \qquad \ldots (28)$$

$$T_0(0) = 0, \qquad T_0(1) = 1, \qquad \ldots (29)$$

$$T_1(0) = 0, \qquad T_1(1) = 0, \qquad \ldots (30)$$

Equations (25) and (26) solve by using the B.C's (29) and (30) we have:

$$T_0(y) = \frac{\mathrm{Sin}\, b_1 y}{\mathrm{Sin}\, b_1}, \qquad (31)$$

$$T_1(y) = 0, \qquad \cdot (32)$$

Putting values from Eqs (31 and 32) in Eq. (16), then we have:

$$T(y,t) = T(y) = \frac{Sinb_1 y}{Sinb_1}, \qquad \ldots \cdot (33)$$

Equations (23) and (24) solve by using the B. C's (27) and (28), and then we have:

$$u_0(y) = c_1 \cosh\sqrt{m_1}\, y + c_2 \sinh\sqrt{m_1}\, y + \frac{a_2}{(b_1^2 + m_1^2)} \frac{\mathrm{Sin} b_1 y}{\mathrm{Sin} b_1}, \qquad \ldots (34)$$

$$u_1(y) = c_3 \cosh\sqrt{m_2}\, y + c_4 \sinh\sqrt{m_2}\, y + \frac{\lambda}{m_2\phi_2}, \qquad (35)$$

Where arbitrary constants are:

$$c_2 = -\frac{a_2}{\sinh\sqrt{m_1}(b_1^2 + m_1^2)},\ c_3 = -\frac{\lambda}{m_2\phi_2}, \qquad \ldots (36)$$

$$c_4 = \frac{\lambda}{m_2\phi_2 \sinh\sqrt{m_2}}(\cosh\sqrt{m_2} - 1), c_1 = 0,$$

Putting values from Eqs (34), (35) and (36) in Eq. (15), then gives:

$$u(y,t) = -\frac{a_2 \sinh\sqrt{m_1}\, y}{(b_1^2 + m_1^2)\sinh\sqrt{m_1}} + \frac{a_2 \sin b_1 y}{(b_1^2 + m_1^2)\sin b_1} +$$

$$\varepsilon e^{i\omega t}\left[\frac{\lambda(\cosh\sqrt{m_2} - 1)\sinh\sqrt{m_2}\, y}{m_2\phi_2 \sinh\sqrt{m_2}} - \frac{\lambda(\cosh\sqrt{m_2}\, y - 1)}{m_2\phi_2}\right] \cdot \ldots (37)$$

Case II: Motion inside a channel with movable top sheet.

Here the top channel sheet ($at\ y = d$) is set into movable flow while the bottom sheet ($at\ y = 0$) is assumed fixed. In this case, the 1st B. C. is the same as in Case- I and the 2nd B. C. in dimensionless form converted to:

$$u(1,t) = H(t)\varepsilon\, \mathrm{e}^{i\omega t}, \quad t > 0, \qquad \ldots (38)$$

Where, $H(t)$ denotes the heaviside unit step function.

Applying a similar process as in Case- I then we have a solution as follows:

$$u(y,t) = -\frac{a_2 \sinh\sqrt{m_1}\, y}{(b_1^2 + m_1^2)\sinh\sqrt{m_1}} + \frac{a_2 \sin(b_1 y)}{(b_1^2 + m_1^2)\sin b_1} + \frac{\varepsilon e^{i\omega t} \sinh\sqrt{m_2}\, y}{\sinh\sqrt{m_2}} \left\{ H(t) + \frac{\lambda(\cosh\sqrt{m_2} - 1)}{m_2\phi_2} \right\} - \frac{\varepsilon e^{i\omega t}\lambda(\cosh\sqrt{m_2}\, y - 1)}{m_2\phi_2} \qquad \ldots (39)$$

Case III: Motion inside a channel with movable top and bottom sheets.

In this case, the channel both sheets are set into fluctuates motions. The dimensionless form of the boundary conditions is:

$$u(0,t) = u(1,t) = H(t)\varepsilon e^{i\omega t}; \quad t > 0 \cdot \qquad \ldots (40)$$

Using the same process as in Case I and the solution is obtained as:

$$u(y,t) = -\frac{a_2 \sinh\sqrt{m_1}\, y)}{(b_1^2 + m_1^2)\sinh\sqrt{m_1}} + \frac{a_2 \sin(b_1 y)}{(b_1^2 + m_1^2)\sin b_1} + \varepsilon e^{i\omega t}\left[\frac{(\cosh\sqrt{m_2} - 1)\sinh\sqrt{m_2}\, y}{\sinh\sqrt{m_2}} \times \left(\frac{\lambda}{m_2\phi_2} - H(t) \right) + \left(H(t) - \frac{\lambda}{m_2\phi_2} \right)\cosh\sqrt{m_2}\, y + \frac{\lambda}{m_2\phi_2} \right] \qquad \ldots (41)$$

3 Nusselt Number and skin-friction

The dimensionless expressions for Nusselt number and skin-frictions are evaluated from Eqs (27, 31, 33 and 35) are as follows:

$$Nu = -\frac{b_1}{\sin b_1}, \qquad \ldots (42)$$

$$\tau_1 = \tau_1(t) = \frac{a_2 m_1}{(b_1^2 + m_1^2)\sinh\sqrt{m_1}} - \frac{a_2 b_1}{(b_1^2 + m_1^2)\sin b_1} + \varepsilon e^{i\omega t}\left[\frac{\lambda(1 - \cosh\sqrt{m_2})}{m_2\phi_2 \sinh\sqrt{m_2}} \right], \qquad \ldots (43)$$

$$\tau_2 = \tau_2(t) = \frac{a_2 m_1}{(b_1^2 + m_1^2)\sinh\sqrt{m_1}} - \frac{a_2 b_1}{(b_1^2 + m_1^2)\sin b_1} + \varepsilon e^{i\omega t}\left[\frac{m_2}{\sinh\sqrt{m_2}} \left\{ H(t) + \frac{\lambda(\cosh\sqrt{m_2} - 1)}{m_2\phi_2} \right\} \right], \qquad \ldots (44)$$

$$\tau_3 = \tau_3(t) = \frac{a_2 m_1}{(b_1^2 + m_1^2)\sinh\sqrt{m_1}} - \frac{a_2 b_1}{(b_1^2 + m_1^2)\sin b_1} + \varepsilon e^{i\omega t}\left[\frac{m_2(\cosh\sqrt{m_2} - 1)}{\sinh\sqrt{m_2}} \left\{ H(t) - \frac{\lambda}{m_2\phi_2} \right\} \right], \qquad \ldots (45)$$

4 Outcome and Conversation

The influence of radiation shows its effects on heat transfer while convection magnetohydrodynamic flow of nanofluids if the porous medium is studied and the channel is filled with nanoparticles. In this paper, three different cases have been discussed based on the boundary conditions. For Al_2O_3, there are four different shapes of nanoparticles which are brick, cylinder, blade, and platelet are dropped into a water-based fluid. The governing PDEs with boundary conditions are solved with the help of using the perturbation technique. Based on Hamilton and Crosser model[26] velocity and temperature expressions are analyzed. Various graphs are discussed in detail and used to consolidate studies of the problem. Table 1 and 2 clarify the values of constants a, b, and sphericity (ψ). Table 3 indicates the numerical

Table 1 – Constants a and b actual shape factors.

Model	a	b
Platelet	37.1	612.6
Blade	14.6	123.3
Cylinder	13.5	904.4
Brick	1.9	471.4

Table 2 – Sphericity ψ for changed shape nano-particles

Model	ψ
Platelet	0.52
Blade	0.36
Cylinder	0.62
Brick	0.81

Table 3 – Thermophsical properties of water and nanoparticles.

Model	H_2O	Cu	TiO_2	Ag	Al_2O_2
$\rho(\kappa g/m)$	997.1	8933	4250	10500	3970
$c_p(\kappa/gK)$	4179	385	686.2	235	765
$\kappa(W/mK)$	0.613	401	8.9528	429	40
$\beta/(10^5K)$	21	1.67	0.9	1.89	0.85

computation for the solution of an equal volume fraction of four different forms of nanoparticles. The velocity profile figures drawn from 1- 21 for all cases and the temperature profile figures drawn from 22 - 25. Figures 1 - 7 are drawn for the case I, Figs 8 - 14 are drawn for the case II and Figs 15-21 are drawn for the case III.

For Al_2O_3, the impact of dissimilar forms of nanoparticles on the momentum of H_2O based nanofluids is drawn in Fig. 1. Figure 1 is drawn to observe the impact of dissimilar forms of Al_2O_3 nanoparticle on the momentum of H_2O based nanofluids. It is evidently noted that the brick shape Al_2O_3 nanoparticles have the highest momentum accompanied by platelet, blade, and cylinder.

In Fig. 2 for Al_2O_3, for cylinder shape nanoparticles, it is clear from the Fig. 2 momentum of nanofluids is reduced if it increases the value of nanoparticle volume fraction ϕ. From this result that the liquid embellishes extra viscous by enhancing the value of nanoparticle volume friction ϕ which guides to reduce the nanofluids momentum. Thermal conductivity of nanofluids as well as increases with the enhances the value of ϕ. Practically this behavior reported by Colla *et al.*[30].

For various values of N are shown in Fig. 3. We noticed that in Fig. 3 the velocity of nanofluids is increased if the value of the radiation parameter N is increased. This analysis owns fine with the outcome gets by Makinde and Mhone[29]. Physically, this means that as N improves, the amount of heat energy transfers to the fluid is improved.

The nanofluids momentum for dissimilar values of M are revealed in Fig. 4. Nanofluid velocity decreases if the value of M increases. Increasing the transverse magnetic field of a conductive fluid produces a resistance called Lorentz force, similar to drag force, and increasing the value of M tends to increase drag force and reduce fluid velocity. Therefore, nanofluid momentum is smallest at the boundaries and highest in the middle of the channel. In Fig. 5, the nanofluids velocity description for

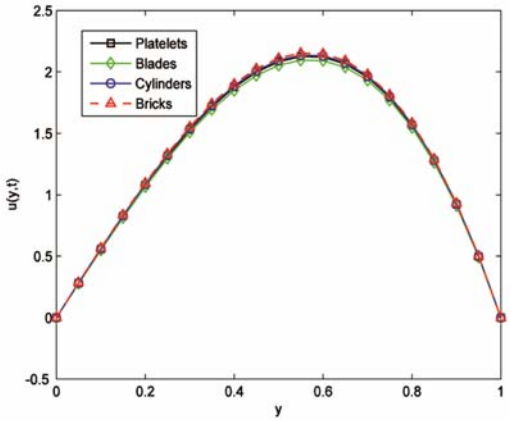

Fig. 1 – Velocity profile of dissimilar shapes of aluminum oxide nanoparticles in H_2O based nanofluid when $M = 1.2, K = 1, \lambda = 1, N = 1, \omega = 0.3, Gr = 0.1,$ $\mathrm{Re} = 5, \phi = 0.03, t = 6, Q = 0.8.$

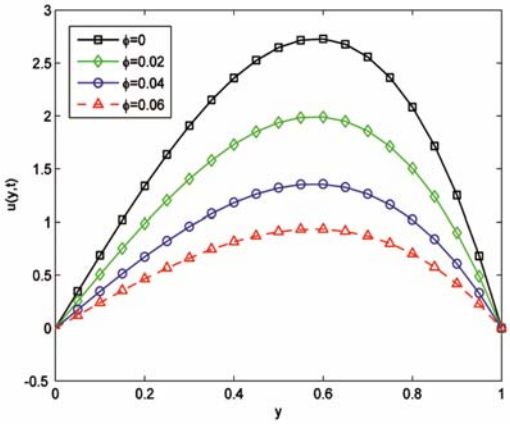

Fig. 2 – Velocity description of unlike values of ϕ in aluminum oxide nanoparticles in H_2O based nanofluid when $M = 1.2, K = 1, \lambda = 1, N = 1, \omega = 0.3, Gr = 0.1,$ $\mathrm{Re} = 5, t = 6, Q = 0.8.$

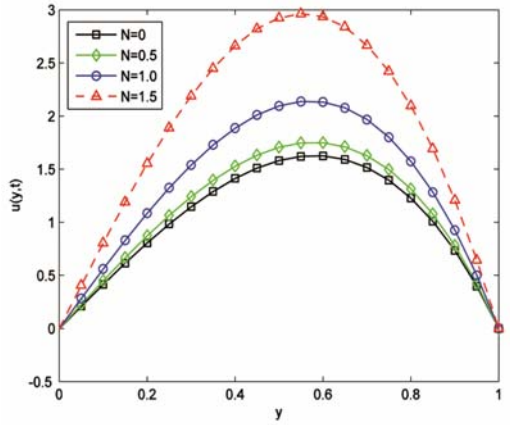

Fig. 3 – Velocity profile of dissimilar values of N in aluminum oxide nanoparticles in H_2O based nanofluid when $M = 1.2, K = 1, \lambda = 0.03, \phi = 1, \omega = 0.3, Gr = 0.1,$ $\mathrm{Re} = 5, t = 6, Q = 0.8.$

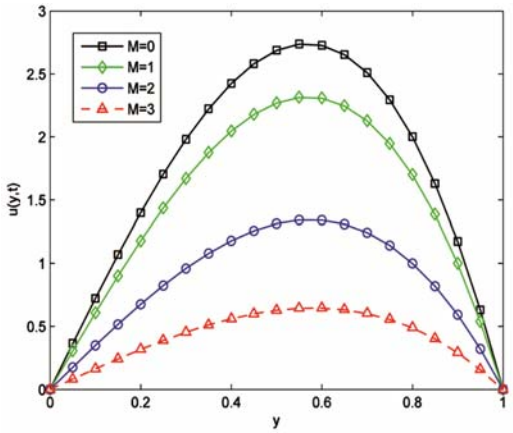

Fig. 4 – Velocity profile of dissimilar values of M in aluminum oxide nanoparticles in H_2O based nanofluid when $N=1$, $K=1$, $\lambda=0.03$, $\phi=1$, $\omega=0.3$, $Gr=0.1$, $\mathrm{Re}=5$, $t=6$, $Q=0.8$.

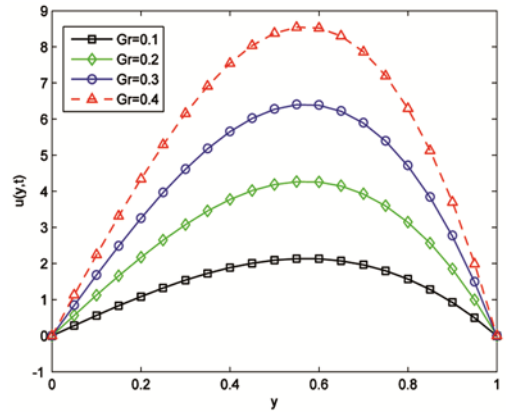

Fig. 5 – Velocity profile of dissimilar values of Grashof number in aluminum oxide nanoparticles in H_2O based nanofluid when $N=1$, $K=1$, $\lambda=0.03$, $\phi=1$, $\omega=0.3$, $M=1.2$, $\mathrm{Re}=5$, $t=6$, $Q=0.8$.

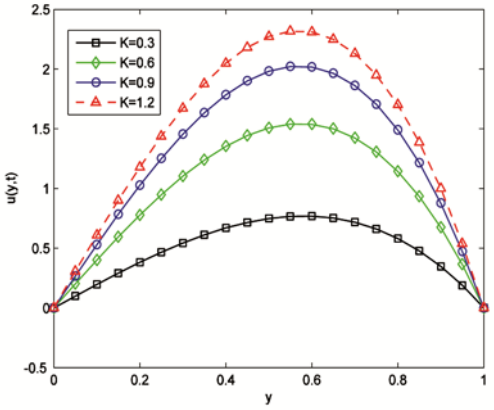

Fig. 6 – Momentum description of dissimilar values of K in Aluminum oxide (Al_2O_3) nanoparticles in H_2O based nanofluid while $N=1$, $Gr=0.1$, $\lambda=0.03$, $\phi=1$, $\omega=0.3$, $M=1.2$, $\mathrm{Re}=5$, $t=6$, $Q=0.8$.

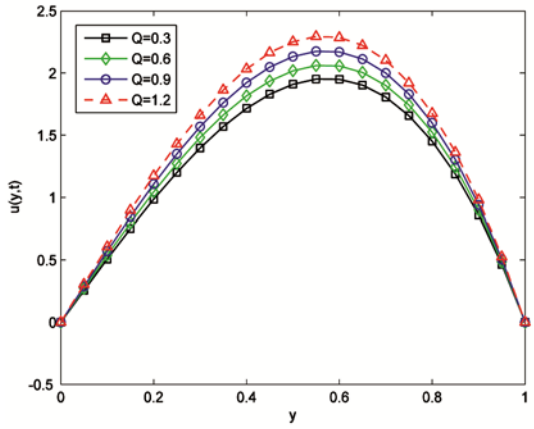

Fig. 7 – Momentum description of dissimilar values of heat source in aluminum oxide (Al_2O_3) nanoparticles in H_2O based nanofluid while $N=1$, $Gr=0.1$, $\lambda=0.03$, $\phi=1$, $\omega=0.3$, $M=1.2$, $\mathrm{Re}=5$, $t=6$, $K=1$.

dissimilar value of Grashof number Gr is shown. We found that the nanofluids velocity enhances if the value of Gr increases. The temperature gradient increases if the value of Gr is increased then the buoyancy force is increased.Therefore, nanofluids momentum enhances arise with Gr, is because of the improvement of buoyancy force. Figure 6 is drawn for porous parameter K. In this figure, we found that if the value of permeability parameter K is increased then the nanofluid velocity increases because of reduced friction force. Further accurately, enhancing permeability parameter K reduces fluid friction by channel partition and momentum increases.

Figure 7 is drawn for a heat source Q. Figure 7 shows that if the value of Q is increases then the nanofluids velocity is increased. This is because, when the heat is absorbed, the buoyancy force increases the speed of the motion.

In the second case, Figs 8 - 14 are drawn for the motion position while the top partition is vibrating and the bottom partition is at rest. Intended the third case, as jointly boundaries bottom and top are vibrating, Figs 15 - 21 are drawn. From the cases second and third, we observed that they are approximately like except altered to Figs 1 - 7.

The impact of distinct shape particles on the temperature of the nanofluid is shown in Fig. 22. The energy in the current investigation is distinct for distinct shapes because of distinct viscosity and thermal conductivity of distinct shapes of nanoparticles. It is observed that the impact of the viscosity decreases as enhance of temperature increases however thermal conductivity increases as

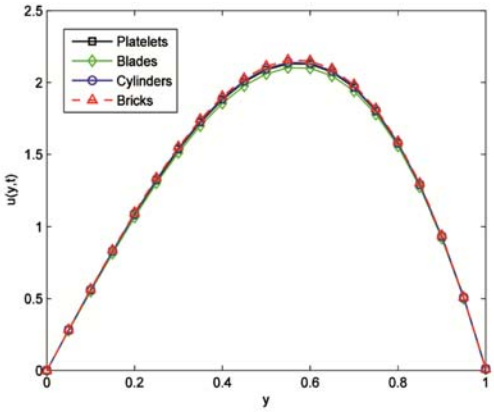

Fig. 8 – Velocity profile of dissimilar shapes of aluminum oxide nanoparticles in H_2O based nanofluid while $M = 1.2, K = 1, \lambda = 1, N = 1, \omega = 0.3, Gr = 0.1,$ $\mathrm{Re} = 5, \phi = 0.03, t = 6, Q = 0.8.$

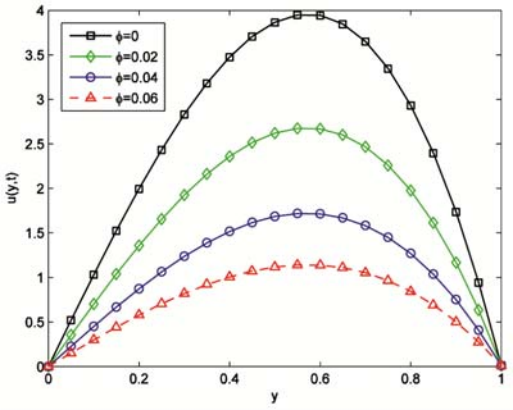

Fig. 9 – Momentum description of dissimilar values of ϕ in aluminum oxide nanoparticles in H_2O based nanofluid while $M = 1.2, K = 1, \lambda = 1, N = 1, \quad \omega = 0.3, Gr = 0.1,$ $\mathrm{Re} = 5, t = 6, Q = 0.8.$

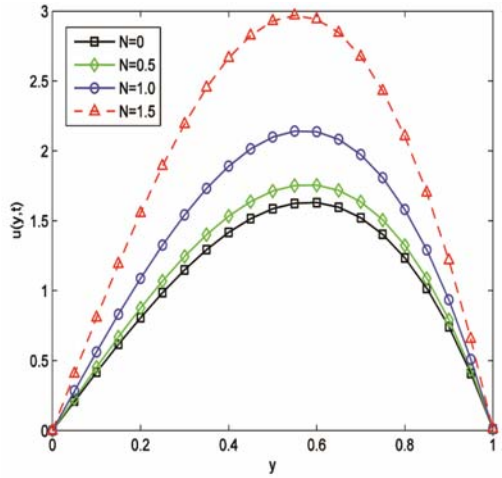

Fig. 10 – Velocity profile of dissimilar values of N in aluminum oxide nanoparticles in H_2O based nanofluid while $M = 1.2, K = 1, \lambda = 0.03, \phi = 1, \omega = 0.3, Gr = 0.1,$

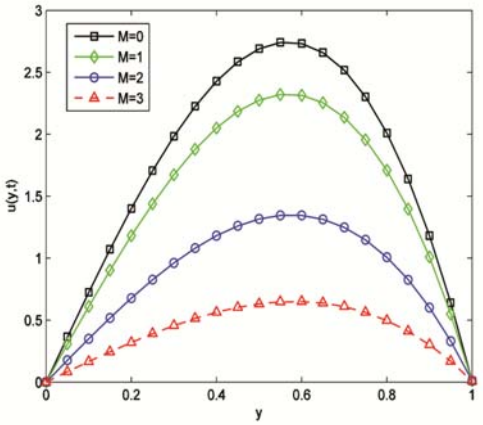

Fig. 11 – Velocity profile of dissimilar values of M in aluminum oxide nanoparticles in H_2O based nanofluid while $N = 1, K = 1, \lambda = 0.03, \phi = 1, \omega = 0.3, Gr = 0.1, \quad \mathrm{Re} = 5,$ $t = 6, Q = 0.8.$

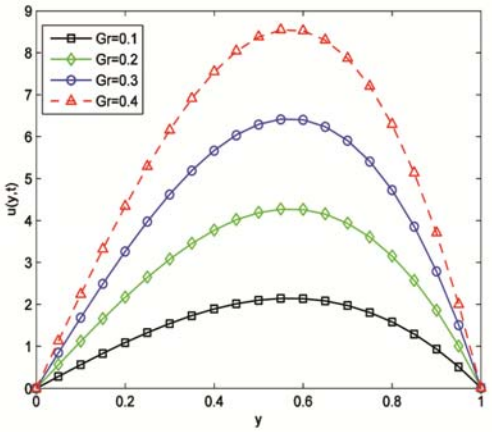

Fig. 12 – Momentum description of dissimilar values of Gr in Aluminum oxide (Al_2O_3) nanoparticles in H_2O based nanofluid when $N = 1, K = 1, \lambda = 0.03, \quad \phi = 1, \omega = 0.3, M = 1.2,$ $\mathrm{Re} = 5, t = 6, Q = 0.8.$

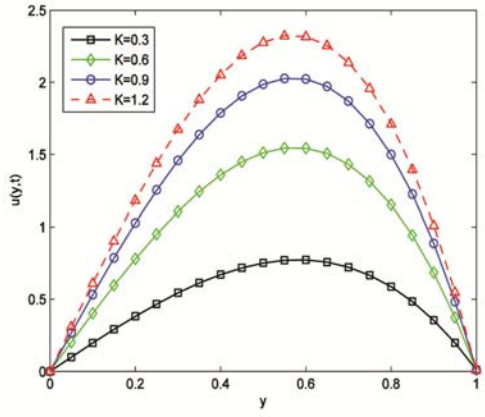

Fig. 13 – Velocity profile of different values of K in aluminum oxide (Al_2O_3) nanoparticles in H_2O based nanofluid while $N = 1, Gr = 0.1, \lambda = 0.03, \phi = 1, \quad \omega = 0.3, M = 1.2, \mathrm{Re} = 5,$ $t = 6, Q = 0.8.$

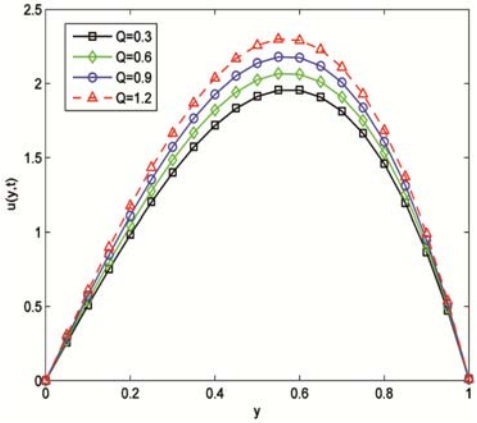

Fig. 14 – Momentum description of dissimilar values of Q in aluminum oxide (Al_2O_3) nanoparticles in H_2O based nanofluid when $N = 1, Gr = 0.1, \lambda = 0.03, \phi = 1, \omega = 0.3, M = 1.2, \text{Re} = 5, t = 6, K = 1.$

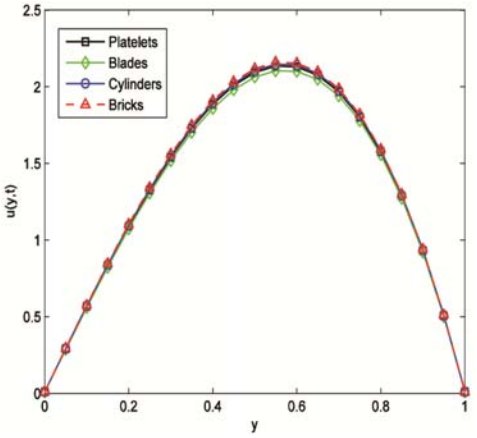

Fig. 15 – Velocity profile of dissimilar shapes of aluminum oxide nanoparticles in H_2O based nanofluid while $M = 1.2, K = 1, \lambda = 1, N = 1, \omega = 0.3, Gr = 0.1, \text{Re} = 5, \phi = 0.03, t = 6, Q = 0.8.$

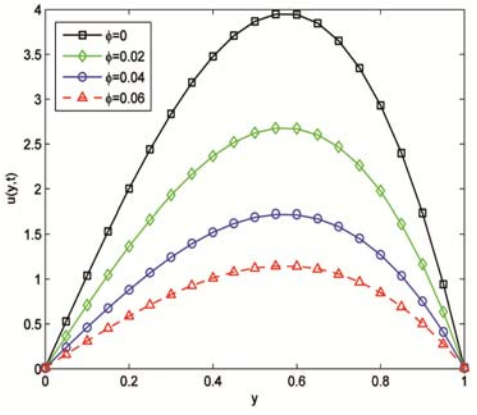

Fig. 16 – Momentum description of dissimilar values of ϕ in aluminum oxide (Al_2O_3) nanoparticles in H_2O based nanofluid when $M = 1.2, K = 1, \lambda = 1, N = 1, \omega = 0.3, Gr = 0.1, \text{Re} = 5, t = 6, Q = 0.8.$

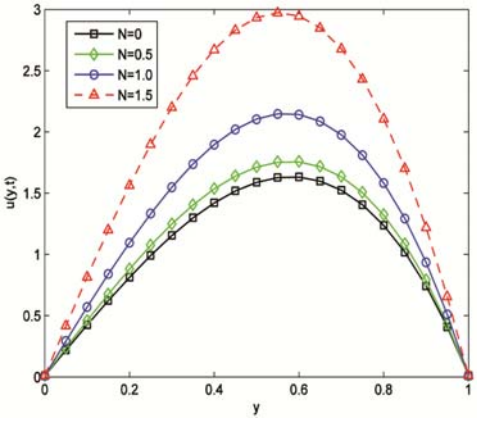

Fig. 17 – Velocity profile of dissimilar values of N in aluminum oxide nanoparticles in H_2O based nanofluid while $M = 1.2, K = 1, \lambda = 0.03, \phi = 1, \omega = 0.3, Gr = 0.1, \text{Re} = 5, t = 6, Q = 0.8.$

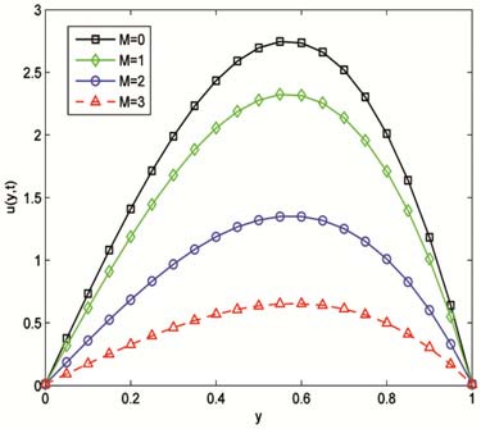

Fig. 18 – Velocity profile of dissimilar values of M in aluminum oxide nanoparticles in H_2O based nanofluid while $N = 1, K = 1, \lambda = 0.03, \phi = 1, \omega = 0.3, Gr = 0.1, \text{Re} = 5, t = 6, Q = 0.8.$

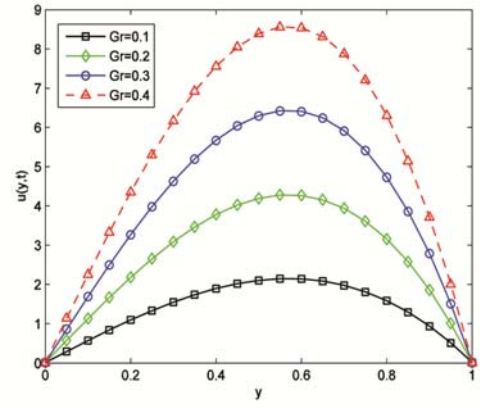

Fig. 19 – Velocity profile of dissimilar values of Gr in aluminum oxide nanoparticles in H_2O based nanofluid while $N = 1, K = 1, \lambda = 0.03, \phi = 1, \omega = 0.3, M = 1.2, \text{Re} = 5, t = 6, Q = 0.8.$

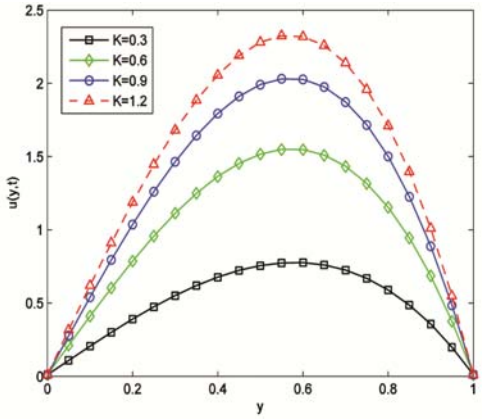

Fig. 20 – Momentum description of dissimilar values of K in aluminum oxide (Al_2O_3) nanoparticles in H_2O based nanofluid when $N=1, Gr=0.1, \lambda=0.03, \quad \phi=1, \omega=0.3, M=1.2, \mathrm{Re}=5, t=6, Q=0.8.$

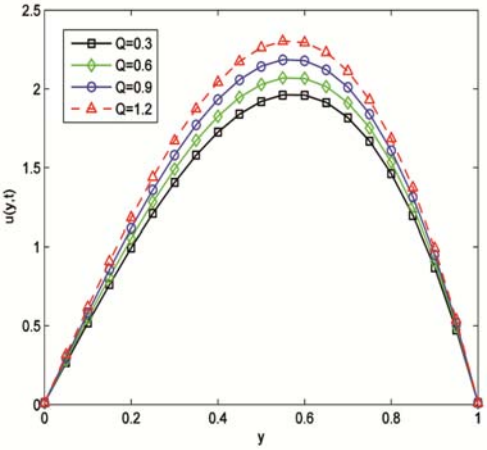

Fig. 21 – Momentum description of dissimilar values of Q in aluminum oxide (Al_2O_3) nanoparticles in H_2O based nanofluid while $N=1, Gr=0.1, \lambda=0.03, \phi=1, \quad \omega=0.3, M=1.2, \mathrm{Re}=5, t=6, K=1.$

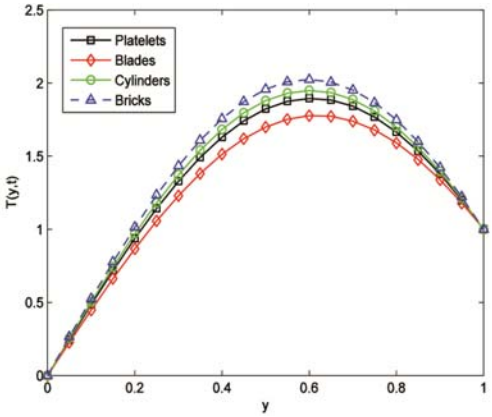

Fig. 22 – Temperature profile of dissimilar shapes of aluminum oxide nanoparticles in H_2O based nanofluid when $N=2, \ \phi=0.02, Q=0.4.$

enhances of temperature. The extended shape of nanoparticles similar to cylinder and platelet has the least temperature on account of the bigger viscosity and thermal conductivity while brick has the maximum energy as a result of slightest viscosity and thermal conductivity. The lowly in energy range brings the blades shape nanoparticles though, it has small viscosity. Figure 23 is drawn to seeing the impact of nanoparticle volume fraction ϕ on the energy profile of the water-based nanofluid. It is clear from the figure if enhances the value of nanoparticles volume fraction ϕ, the temperature profile of the nanofluid decreases. Figure 24 is drawn for seeing the effect of different values of radiation parameter N. In this figure, we show that if increasing the value of the radiation parameter N, the cylinder shape

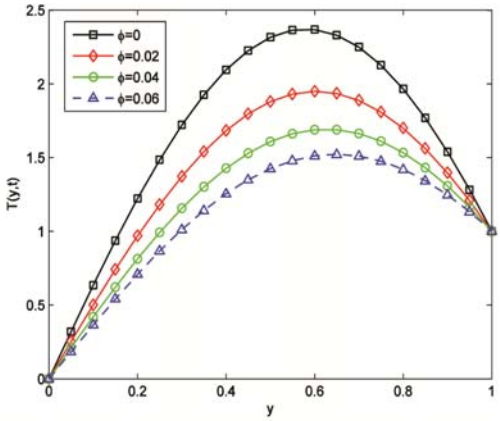

Fig. 23 – Temperature profile of dissimilar values of ϕ in aluminum oxide (Al_2O_3) nanoparticles in H_2O based nanofluid while $N=2, Q=0.4.$

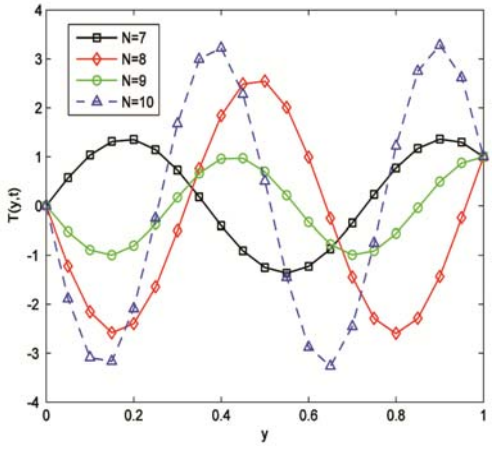

Fig. 24 – Energy description of dissimilar values of N in aluminum oxide (Al_2O_3) nanoparticles in H_2O based nanofluid while $\phi=0.02, Q=0.4.$

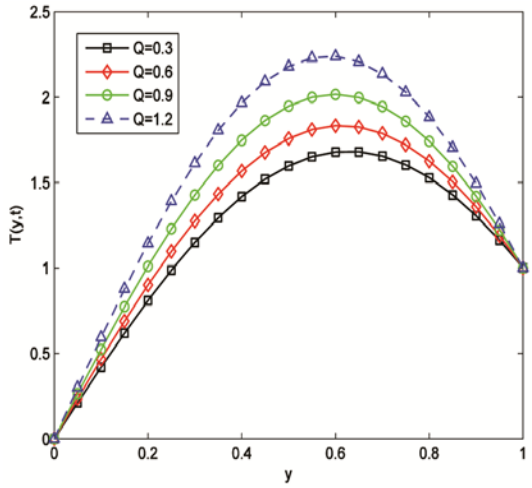

Fig. 25 – Energy description of dissimilar values of Q in aluminum oxide (Al_2O_3) nanoparticles in H_2O based nanofluid while $\phi = 0.02$, $N = 2$.

nanoparticles in water-based nanofluid obtain an additional curvilinear profile for the temperature profile. Figure 25 is drawn for seeing the effect of different values of the heat source Q. In this figure, we show that if increasing the value of Q, the temperature profile of the nanofluid increases. As the Q increases, more heat is generated. As a result, the speed of the nanofluid increases.

5 Conclusions

In the current work, the impact of radiation transport of heat in the combined convective magnetohydrodynamic motion of dissimilar shapes of Al_2O_3 in the H_2O-based nanofluids in a waterway packed via flooded permeable media are analyzed. The waterway through non-uniform partition temperature is in use in a perpendicular direction with the impact of a transverse magnetic field. Using the perturb method for three dissimilar motion conditions, the governing PDEs are solved and analytic outcomes are attained. The impact of the dissimilar shapes of nanoparticles specifically platelet, blade, cylinder, and brick of identical volume on the momentum and energy of nanofluids are the resolution by means of diverse results. This work studies the shear-thinning performance of cylinder and blade form of nanoparticles. The concluded remarks are as follows:

(i) Increases the values of volume fraction of nanoparticles because of the enhance of viscosity and thermal conductivity, the nanofluid momentum is decreasing,

(ii) Nanosize particles instance platelet and blade shapes have lesser momentum as related to brick and cylinder size of nanoparticles,

(iii) Nanofluid velocity increases with the increase of radiation parameter,

(iv) The momentum of the nanofluid increases by means enhance of permeability variable, and

(v) The velocity of the nanofluid and temperature increases with the increase of heat source.

Acknowledgment

The authors are grateful to Prof G C Sharma, Agra University, Agra, India for his help and valuable suggestions to prepare this research paper and thanks to reviewers also.

Nomenclature:

List of Symbols:

B_0	Strength of applied magnetic field;
c_p	Specific heat;
$(c_p)_s$	Specific heat of solid nanoparticles at Constant pressure;
$(c_p)_f$	Specific heat of base fluid at constant pressure;
d	Distance between plates ;
Gr	Thermal Grashof number;
g	Acceleration due to gravity;
K	Permeability parameter;
k_1	Porous medium permeability;
k_{nf}	Thermal conductivity;
M	Magnetic parameter;
N	Radiation parameter;
p	Pressure;
$\tilde{p}$	Dimensionless pressure;
Pe	Peclet number;
Q	Heat source parameter;
q	Radiative heat flux;
Re	Reynolds number;
T	Temperature;
$\tilde{T}$	Dimensionless temperature;
T^*	Temperature at $y = 0$;
T_w	Temperature at $y = d$;
t	Time;
$\tilde{t}$	Dimensionless time;
u	Velocity component in the direction of the $x-$axis;

$\tilde{u}$ Dimensionless velocity;
U_0 Velocity of the plate;
x Coordinate axis along with the flow;
$\tilde{x}$ Dimensionless axis along with the flow;
y Coordinate axis normal to the plate;
$\tilde{y}$ Dimensionless axis normal to the plate;

Greek Symbols

α Radiation absorption coefficient;
β Thermal expansion coefficient;
β_s The thermal expansion coefficient of solid nanoparticles;
β_f The thermal expansion coefficient of base fluids;
σ Electrical conductivity;
ϕ Nanoparticles volume fraction;
ν_f Kinematic viscosity of the fluid;
ρ_{nf} Density of nanofluid;
ρ_f Density of base fluid;
ρ_s The density of solid nanoparticles;
$(\rho\beta)_{nf}$ Nanofluid thermal expansion coefficient;
$(\rho c_p)_{nf}$ Heat capacitance of nanofluid;
$(\rho c_p)_f$ Heat capacitance of base fluid;
$(\rho c_p)_s$ Heat capacitance of nanoparticle;
μ_{nf} The viscosity of nanofluid;

References

1 Choi S U S, Siginer D A & Wang H P, *ASME, New York,* 66 (1995) 99.
2 Mansur S, Ishak A & Pop I, *PLOS One*, 10 (2015) 1.
3 Ellahi R, Hassan M & Zeeshan A, *Int J Heat Mass Trans,* 81 (2015) 449.
4 Sheikholeslami M, Ganji D D & Javed M Y, *J Magn Magn Mater*, 374 (2015) 36.
5 Rashidi S, Dehghan M, Ellahi R, Riaz M & Jamal-Abad M T, *J Magn Magn Mater,* 378 (2015) 128.
6 Noreen S A, Raza M & Ellahi R, *Eur Phys J Plus*, 129 (2014) 185.
7 Ellahi R, Hassan M & Soleimani S, *Int J Num Meth Heat Fluid Flow*, 24 (2014) 1906.
8 Sheikholeslami M, Ellahi R, Ashorynejad H R, Domairry G & Hayat T, *Comput Theor Nano*, 11 (2014) 486.
9 SheikholeslamI M, Bandpy M G, Ellahi R & Zeeshan A, *J Magn Magn Mater*, 369 (2014) 69.
10 Noreen S A, Rahman S U, Ellahi R & Nadeem S, *Int J Therm Sci*, 85 (2014) 54.
11 Ellahi R, *Appl Math Mod*, 37 (2013) 1451.
12 Wang X B, Zhou P L & Peng F X, *Int J Heat Mass Trans,* 46 (2003) 2665.
13 Aiza G, Khan I & Shafie S, *Nanoscale Res Lett*, 10 (2015) 490.
14 Timofeeva E V, Jules R L & Dileep S, *J Appl Phys*, 106 (2009) 014304.
15 Loganathan P, Chand P N & Ganesan P, *NANO*, 8 (2013) 1350001.
16 Asma K, Khan I & Sharidan S, *Eur Phys J Plus*, 130 (2015) 57.
17 Sebdani S, Mahmoodi M & Hashemi S, *Int J Therm Sci*, 52 (2012) 112.
18 Fan T, XU H & Pop I, *Int J Spr plus,* 34 (2013) 339.
19 Tiwari R K & Das M K, *Int J Heat Mass Trans*, 50 (2007) 9.
20 Sheikhzadeh G A, Hajialigol N, Qomi M E & Fattahi A, *J Nano*, 1 (2012) 44.
21 Nadeem S & Saleem S, *Appl Nano*, 4 (2014) 405.
22 Al-Salem K, Oztop H F, Pop I & Varol Y, *Int J Heat Mass Trans*, 55 (2012) 1103.
23 Prasad K V, Vajravelu K & Datti P S, *Int J Ther Sci,* 49 (2010) 603.
24 Rami J Y, Fawzi A & Abu-Al-Rub F, *Int J Num Meth Heat Fluid Flow*, 11 (2011) 600.
25 Hayat T, Abbas Z, Pop I & Asghar S, *Int J Heat Mass Trans*, 53 (2010) 466.
26 Hamilton R L & Crosser O K, *J Ind Eng Chem Fund*, 1 (1962) 187.
27 Turkyilmazoglu M, *Int J Heat Trans*, 136 (2014) 031704.
28 Zeehan A, Ellahi R & Hassan M, *Eur Phys J Plus*, 129 (2014) 261.
29 Makinde O D & Mhone P Y, *Romanian J Phys*, 50 (2005) 931.
30 Colla L, Fedele L, Scattolini M & Bobbo S, *Ad Mech Eng A,* 8 (2012) 674947.
31 Noreen A S, Raza M & Ellahi R, *J Magn Magn Mater*, 381 (2015) 405.
32 Ellahi R, Aziz S & Zeeshan A, *J Porous Media*, 16(3) (2013) 205.
33 Noreen A S, Raza M & Ellahi R, *Eur Phys J Plus*, 129 (2014) 155.
34 Sheikholeslami M & Ellahi R, *Int J Heat Mass Trans,* 89 (2015) 799.
35 Ellahi R, Hassan M & Zeeshan A, *IEEE Trans Nanotechnol,* 14(4) (2015) 726.
36 Sheikholeslami M & Ellahi R, *J Zeit Fur Naturf,* 70 (2015) 115.
37 Ibrahim S M, Lorenzini G, Vijaya Kumar P & Raju C S K, *Int J Heat Mass Trans,* 111 (2017) 346.
38 Nandy S K & Mahapatra T R, *Int J Heat Mass Trans,* 64 (2013) 1091.
39 Hayat T, Qayyum S, Alsaedi A & Shafiq A, *Int J Heat Mass Trans,* 103 (2016) 99.
40 Kundu P K, Das K & Jana S, *Afrika Mat*, 25(2) (2014) 363.
41 Das K, *Appl Math Comput*, 221 (2013) 547.
42 Madhu M & Kishan N, *J Appl Mech Tech Phys*, 57(5) (2016) 908.
43 Naramgari S & Sulochana C, *Ain Shams Eng J*, (2016) in press.